Measurement of (n,*x*nγ) reaction cross sections in W isotopes

G. Henning[1,2], *A. Bacquias*[1,2], *C. Dorcea*[3], *P. Dessagne*[1,2], *J.-C. Drohé*[4], *M. Kerveno*[1,2], *A. Negret*[3], *M. Nyman*[4], *A. Olacel*[3,5], *A.J.M. Plompen*[4], *G. Rudolf*[1,2], *P. Scholtes*[1,2]

[1] Université de Strasbourg, IPHC, Strasbourg, France. [2] CNRS, UMR7178, 67037 Strasbourg, France. [3] Horia Hulubei National Institute for Physics and Nuclear Engineering, Bucharest-Magurele, Romania. [4] European Commission, Joint Research Center, Institute for Reference Materials and Measurements, B-2440 Geel, Belgium. [5] University of Bucharest, Faculty of Physics, Bucharest-Magurele, Romania.

Abstract

Nowadays, most of nuclear reactor developments use evaluated databases for numerical simulations to optimize reactors performance and control parameters. However, the considered databases present still large uncertainties and disagreements, preventing calculations from reaching the required precision. The necessary improvement of evaluated databases entails new measurements and a better theoretical description of involved reactions. Among those, the neutron inelastic scattering (n, *x*n) is of great importance as it modifies the neutron spectrum, the neutron population, and produces radioactive species. In 2005, the group at IPHC started an experimental program to study these reactions. The setup and the analysis will be presented along with the first results for natural tungsten isotopes, which will be compared to the latest predictions from nuclear reaction codes. The impact of those results on reaction mechanism description will be discussed.

1. Motivation

Today most of the nuclear reactor developments are using evaluated data bases for numerical simulations. These data bases contain all necessary quantities for the simulations: total and partial cross sections, angular distributions, ... However, the considered databases still present large uncertainties and disagreements. To improve their level of precision, new measurements and theoretical developpements are needed.

The (n, *x*n) reactions are of particular interest as they modify the neutron spectrum, the neutron population, and produce radioactive species. This type of reaction occurs purely via nuclear interaction between the incomming neutron and the nucleons, which makes them a good probe of this interaction. Moreover, the neutron inelastic scaterring proceeds through three main mechanisms: direct nucleon-nucleon interaction for the highest neutron energy, compound nucleus for the slow neutrons with a long interaction time with the nucleus and pre-equilibrium reactions, for intermediate energy, in which the incoming neutron interacts with several but not all the nucleons. These three reaction regimes are described differently by the theories but overlap in reality.

To experimentally extract the total (n, *x*n) cross section, the study of the exclusive channels (n, *x*nγ) brings very strong constrains for the comparison with theoretical predictions as such calcualtion requires a correct description of the reaction mechanism, the nuclear de-excitaiton process and the precise knowledge of the nuclear strucutre. The group at IPHC started a program to study (n, *x*nγ) reaction on actinides in 2005 and already worked on ^{235,238}U and ^{232}Th [1, 2], while measurements for other elements were performed and are being analysed, including ^{nat}W.

In the following, we report on the study done on tungsten isotopes ($^{182-186}_{74}$W). Tungsten is not an active element in nuclear reactors. However, with a high melting point (3422 °C), a strong mechanical resistance (Young's modulus: 600 GPa) [3], a low thermal expansion and a high resistance to oxidation,

acids and alkaline, it is used in many alloys. The interaction of neutrons with tungsten is therefore of importance for reactor physics, in particular for fusion reactors in which tungsten is one of the most exposed material to high energy neutrons [4]. Compared to actinides, the setup of experiments using tungsten is very simple as the metal is not radioactive and does not have any toxicity.

From the structure point of view, tungsten isotopes are similar in deformation to actinides such as Uranium, as illustrated on 1. This similarity comes with the simplification, compared to actinides, that tungsten isotopes do not present a neutron-induced fission channel (the calculated liquid drop fission barrier of tungsten isotopes is around 20 MeV [5]).
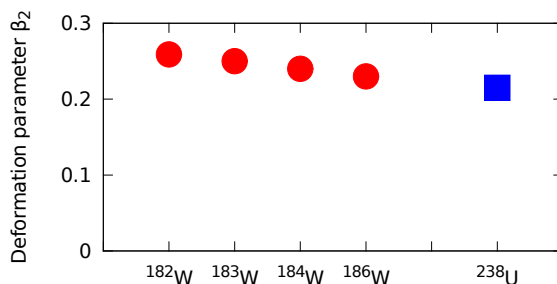

Fig. 1: Calculated ground-state deformation parameters for ^{182,183,184,186}W and ^{238}U [5].

As the nuclear applications do not use isotopically enriched isotopes, one has to study all the naturally abundant isotopes: ^{182}W (26.5 %), ^{183}W (14.3 %), ^{184}W (30.6 %), ^{186}W(28.4 %) [6].

Moreover, there are only a few measurements available today on these nuclides to test evaluations. Some (n, 2n) and (n, 3n) cross section data exist, and a few (n, n') level production cross sections have been measured [22, 7, 8].

2.   Experimental setup: GRAPhEME@GELINA

Experimental measurements of (n, xnγ) reaction cross sections using prompt gamma spectroscopy and neutron energy determination by time of flight are performed at the neutron beam facility GELINA, at the European Commission Joint Research Center's Institute for Reference Materials and Measurements in Geel, Belgium [9, 10].

The GELINA accelerator provides a pulsed neutron white beam using electrons accelerated at 100 MeV impacting a uranium target. The accelerated particles produce Bremsstrahlung radiations in the uranium target which in turn, by photonuclear reactions, produce neutrons, with an average flux of 3.4×10^{13} neutrons/s. The neutron energy distribution ranges from subthermal to about 20 MeV, with a peak around 1-2 MeV. The flight paths, symmetrically arranged around the uranium target, lead to several experimental locations at distances of 10 to 400 m. For each fligth path, a different set of moderators can be added to modify the neutron spectrum.

The GRAPhEME setup is located 30 meters away from the neutron production target and consists of a fission chamber (FC) to measure the incoming neutron flux and HPGe detectors for the detection of γ rays. The FC is a $\approx 320\,\mathrm{cm}^3$ volume, filled with a 10 % methane- and 90 % argon-mixture at 1 atm pressure, with a ^{235}U enriched (99.5 %) UF_4 deposit. The reaction of neutrons with the ^{235}U nuclei induces fission and one of the fission fragment is detected in the gas chamber. The efficiency of the FC was determined to be 94.4 ± 2.1 % [11, 12]. An energy cut allows the differentiation between α particles and fission fragments.

After the fission chamber, planar HPGe detectors surround the sample to study. The average resolution of the detectors at 122 keV is 0.75 keV and the absolute efficiency is 0.01. The sample

and the detectors are enclosed into a lead-copper-cadmium castle to drastically reduce the background around the target.

The detectors are connected to TNT acquisition cards [13] that record in list mode the energy of the detected gamma ray (or fission fragment) and the time of the event. The time difference between the accelerator pulse and the γ-ray or fission event detection gives the energy of the neutron that induced the reaction, following $E_n = m_n c^2 \sqrt{\frac{1}{1-\left(\frac{D/T}{c}\right)}}$ where m_n is the mass of the neutron, c the speed of light in vacuum, D the neutron flight path length between the production target and the sample in GRAPhEME and T is the time of flight of the neutron.

To extract cross section at a given angle θ and neutron energy E_n, one simply has to follow the intensity of a given gamma ray line detected by the HPGe detectors and make a ratio with the neutron flux determined by the fission chamber according to the following equation:

$$\frac{d\sigma}{d\Omega}(E_n, \gamma; \theta) = \frac{N_\gamma(E_n; \theta)}{\varepsilon(E_\gamma)} \frac{\sigma_{235_{U(n, f)}}(E_n)\varepsilon_{FC}}{N_{target}N_{FC}}$$

Where $N_\gamma(E_n; \theta)$ is the number of detected γ rays for a given transition, $\varepsilon(E_\gamma)$ the efficiency of detection for this γ ray, $\sigma_{235_{U(n, f)}}(E_n)$ the fission induced cross section of ^{235}U, ε_{FC} the detection efficiency of the fission chamber, N_{target} the number of isotope of interest in the sample and N_{FC} the number of events detected by the fission chamber.

The full angular integration is made using the Gauss quadrature method with detectors positioned at 110 °and 150 ° [14, 15].

Measurements of (n, xn γ) cross sections have been performed for ^{nat,182,183,184,186}W targets. Here only the preliminary results for the even-even isotopes studied in a ^{nat}W target are presented.

3. Results

The structure of the three isotopes ^{182,184,186}W is very similar, with a strong rotor-like behavior. The yrast states form a rotational band built on the 0^+ ground state. The moment of inertia $\mathscr{J}_{yrast}$ is decreasing slightly with the increase of the neutron number (N). The nuclei also present a 2^+-based band (γ) and a 0^+-based band (β). As N increases, the 2^+-based band is being lowered below the 0^+-based band. See 2 for the level schemes.
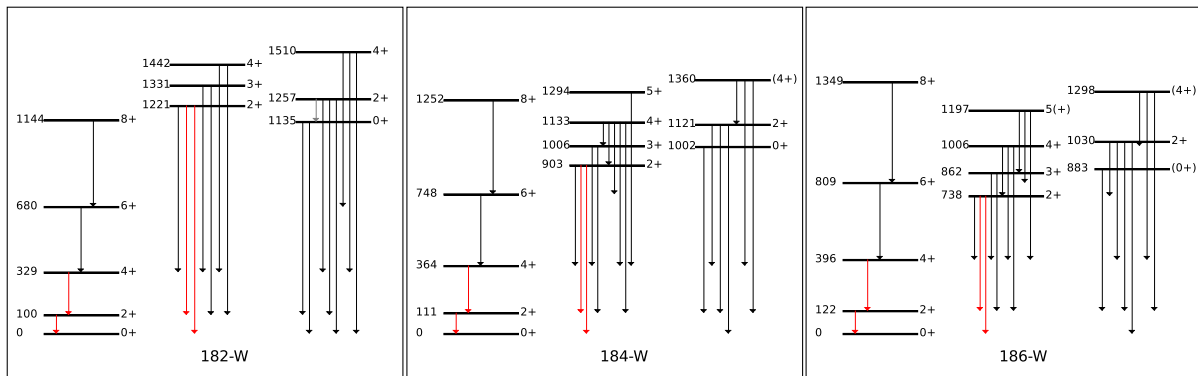

Fig. 2: Level schemes of ^{182,184,186}W [16, 17, 18]. The energy of levels are given in keV. The transitions in red are the ones that will be discussed here.

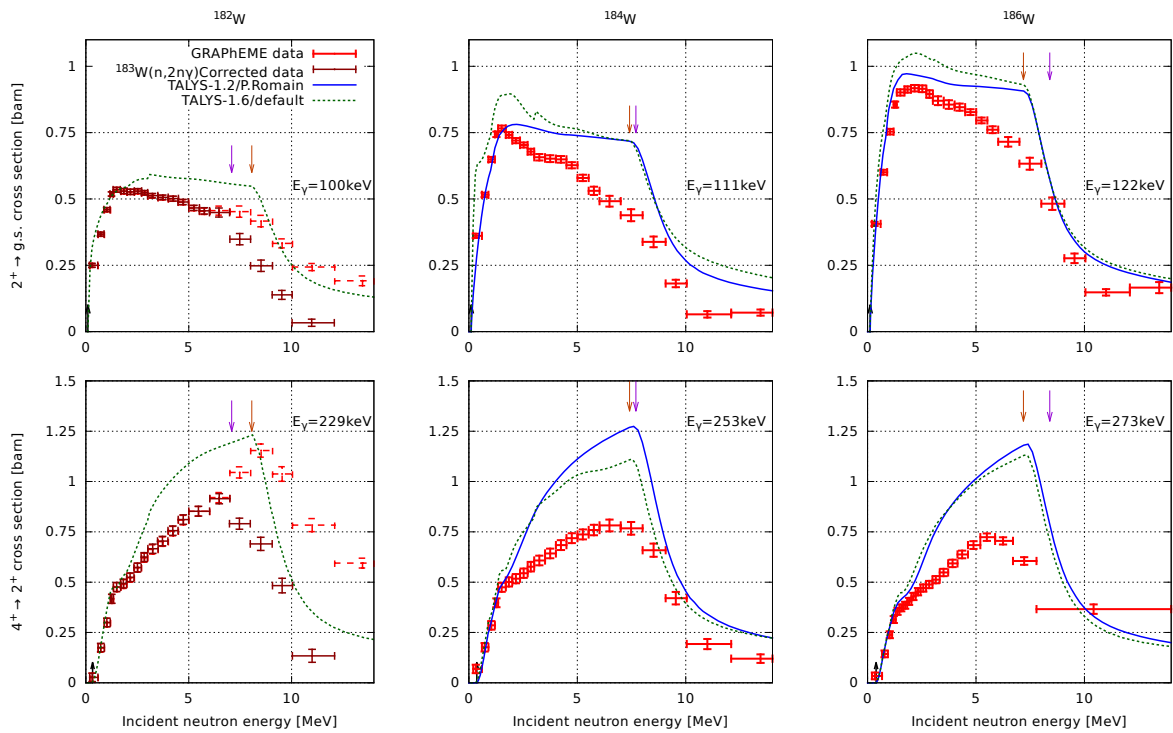**Fig. 3:** (n, n'γ) cross sections measured with GRAPhEME (red points) for the isotopes ^{182}W (left), ^{184}W (center), ^{186}W (rigth), for the first excited state to the ground state transition (top) and the second excited state to the first excited state (bottom). The data is compared to TALYS-1.2 calculation with optimized parameters (full blue line) and with TALYS-1.6 with default parameters (dotted green line). For references, the energy of the level from which the γ rays are decaying is marked with the black up-pointing arrow. The neutron separation energy S_n is marked with the orange down-pointing arrow, the proton separation energy S_p by the purple down-pointing arrow.

3.1   Ground state band transitions

First, we look at the transitions, in the ground state band, from the 4^+ to the 2^+ level and from the 2^+ to the *g.s.*. For ^{182}W(n, n'γ) it is necessary to correct for the contamination by ^{183}W(n, 2n) reactions in the natural W target. This is done by substracting the ^{183}W(n, 2nγ) transition cross section calculated with TALYS-1.6, weighted by the isotopic ratio in natural tungsten. The profile of the cross sections (3) is very similar for the transitions along the isotopic chain. For the 2^+ to *g.s.* transition, the cross section peaks around $E_n = 1 - 2$ MeV, and starts dropping above 6 MeV. For the 4^+ to 2^+ transition, the cross section increases sharply from 0 to 500 keV, has a *softer* slope above, peaks around $6 - 8$ MeV and drops just above the peak. In terms of amplitude, the maximum of the cross section for the 2^+ to *g.s.* appears to increase with larger neutron number. The 4^+ to 2^+ cross section amplitude, is sligthly decreasing for increasing N. However, one should not be fooled by electron conversion. Indeed, for the W isotopes, the conversion coefficient for transitions around 100 keV is about 3, and about 0.2 for transitions around 250 keV. Correcting for conversion electrons, the 2^+ to *g.s.* transition cross sections are very similar at ≈ 2.5 barns. The 4^+ to 2^+ transition represents only about 1/3 of the 2^+ to *g.s.* transition at $E_n \approx 2 - 5$ MeV. At the highest neutron energy, most of the 2^+ to *g.s.* intensity comes from the 4^+ to 2^+. This indicates a weak contribution from the ground state band to the 2^+ level population.

The experimental cross sections are compared to predictions by the TALYS code (shown in 3). Two TALYS calculations were performed. The first one was made in 2011 by P. Romain (CEA/DAM) with TALYS-1.2 and optimized parameters for ^{184,186}W. The second was performed with the latest

TALYS version (1.6) with default parameters for all three isotopes. We note that TALYS-1.2 calculations using default parameters give values within 3 % of the TALYS-1.6 default results. The experimental data and the TALYS predictions match very well at low energy ($E_n < 1$ MeV) but start to differ above. In the 2^+ to *g.s.* transitions TALYS predicts a plateau from $E_n \approx 2$ MeV to ≈ 8 MeV (i.e. at the neutron separation energy) while the experimental data drops already starting at 6 MeV. In the 4^+ to 2^+ transition, TALYS overestimates the intensity of the transition from 2 to 8 MeV, by as much as a factor 2.

3.2   Interband transitions

The two transitions decaying from the 2_2^+ state (head of the γ band) are also studied. This state decays to the 2_1^+ state in the ground state band and to the ground state – it also decays to the 4_1^+ state but with a very low branching ratio) – see 4. For the ^{182}W, the transitions are contaminated by other γ lines and hard to isolate in the spectrum. In the two other isotopes (^{184,186}W), the transitions have very similar shapes and amplitudes, in agreement with the expectations. Electron conversion is negligible at this γ energy. Comparing to predictions by TALYS, the calculations reproduce very well the shape of the cross sections. However, the amplitude is underestimated by as much as ≈ 25 %.
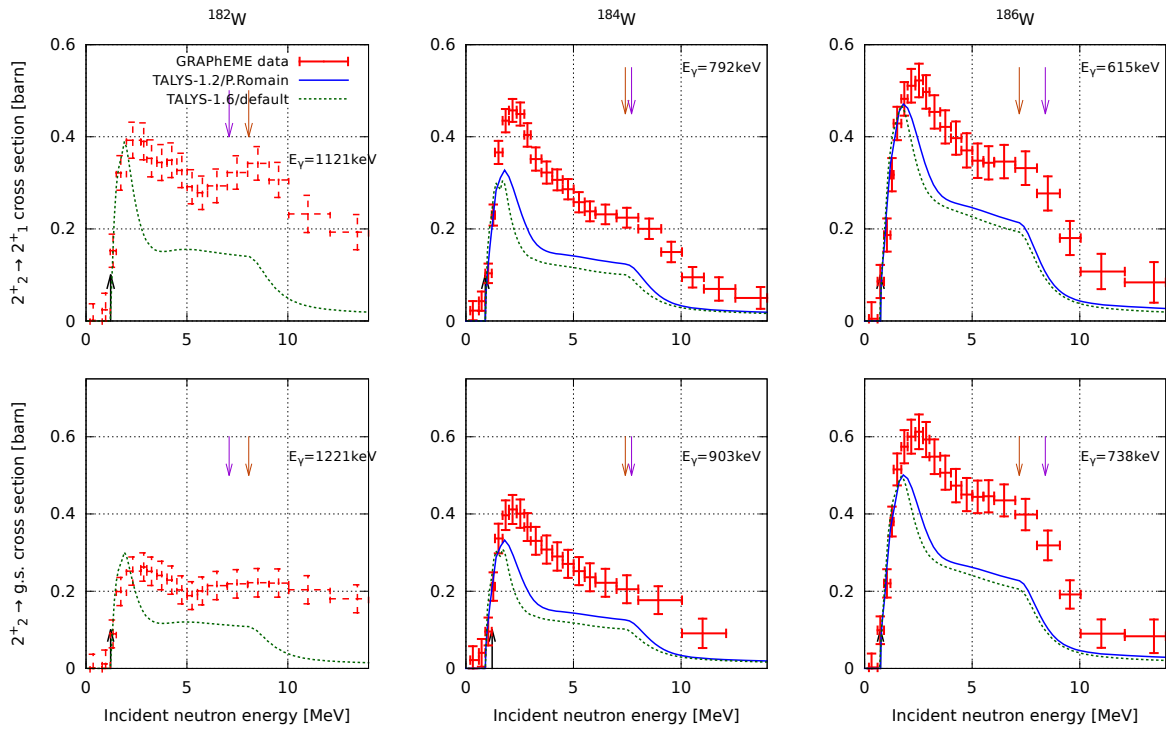

Fig. 4: Same as 3 for interband transitions decaying from the 2^+ band. Data for ^{182}W is unreliable because of γ contamination.

4.   Result interpretation

Significant differences appear between the experimental results and the theoretical predictions. TALYS overestimates the ground state band intensity for the higher E_n, and underestimates the interband transitions intensity at all neutron energies.
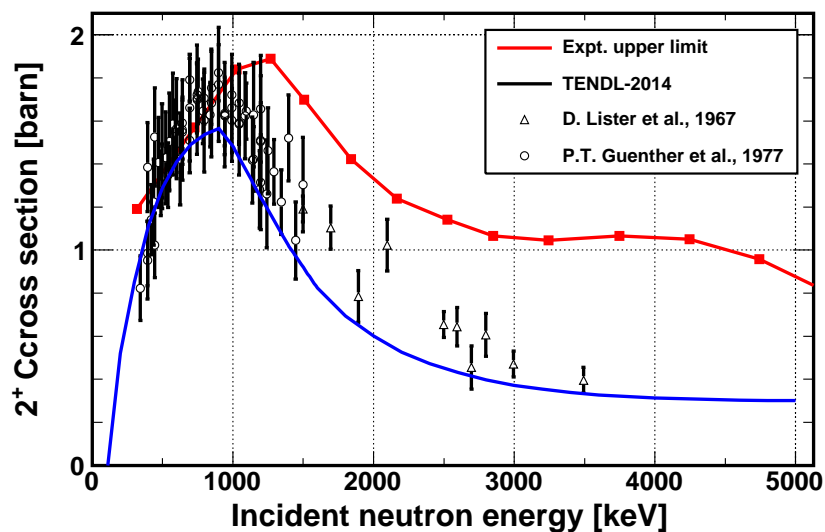
Fig. 5: Level poppulation cross section for the first excited state (2^+) in ^{184}W. The red line is the upper limit determined from GRAPhEME data. The markers are from available experimental data [22, 7, 8]. The blue line is the value in TENDL-2014 [19, 20].

A possible explanation is incorrect branching ratios in the structure information used by TALYS. To extract information that is independant of branching ratio, we tried to extract the 2^+ level population cross section from the γ cross sections. This relies on the balance formula: $\sigma_{\text{level}} = \sum_{\text{decaying transition}} \sigma_{\text{transition}} - \sum_{\text{feeding transition}} \sigma_{\text{transition}}$. With this method, it is important to correct the transition intensity extracted from γ ray intensity for the electron conversion. Although simple in principle, the extraction of the 2^+ level population cross section from gamma transition intensity is tricky. Indeed, for ^{184}W, more than 20 transitions are feeding the first excited state; many of which have a high energy, for which our setup has a low efficiency, with a highly fractionned intensity. Because of this difficulty, the level population cross section can be extracted exactly only up to 1 MeV, and only an upper limit can be determined above that energy – see 5. The comparison of the upper limit extracted from experimental data with previous data existing for the level cross section, and the TALYS prediction, show a good agreement of our data with previous experiments, but can not allow to draw further conclusions.

Another lead to explain the difference between TALYS and the experimental data is the description in the calcualtions of the reaction mecanism. P. Romain decomposed the total ^{186}W(n, n' $\gamma_{2^+ \to \text{g.s.}}$) according to individual state contributions. The computed cross section is a good match to the experimental data from a previous analysis of the same data set presented in the current paper, with only a small renormalization. This description is very good up to 4 MeV. This is hinting that the structure information used by TALYS is good enough up to the high excitation energies. Above 5-6 MeV, the plateau predicted by TALYS, associated with scaterring off continuum states continues while the experimental data is dropping. This can be explained by an incorrect description of the spin distribution from pre-equilibrium reactions, as it has been seen in U isotopes [21]. For this aspect, microscopic calculation done by M. Dupuis (CEA/DAM) could be a way to obtain correct spin distributions. In general, one can also wonder about the choice of the energy limit between continuum and discrete levels and the coupling between them.
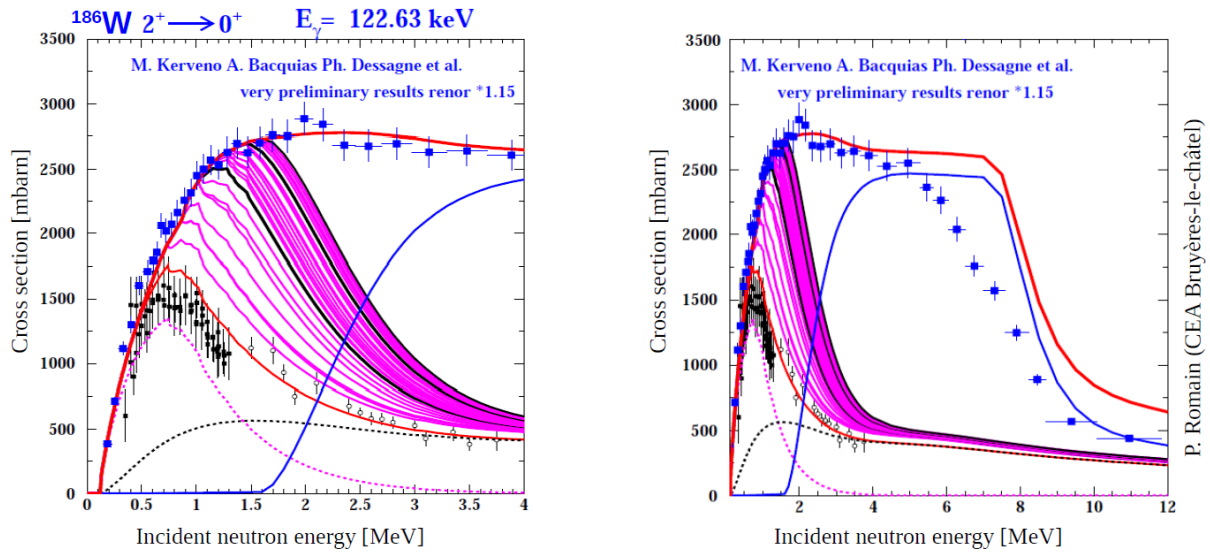
Fig. 6: Decomposition of the ^{186}W(n, n' $\gamma_{2^+\rightarrow g.s.}$) cross section according to the individual levels. The cumulative contributition of the 2^+ level is in thin red line (with the direct component in dotter black and the CN component in dotted purple). For comparison, the experimental data from [7, 8, 22] are indicated. The contribution of other levels, appropriately weighted by branching ratios are in continuous purple and black lines. The contribution of the continuum is in continuous blue. The total is the thick red line, compared to scaled data from a previous analysis (see text).

5.   Conclusion and perspectives

From the preliminary results of (n, xnγ) cross sections measured on ^{182,184,186}W, we see that TALYS overestimates the cross section of transitions in the ground state band, while it under estimates the interband transitions intensity. The shape of the 2^+ to *g.s.* transition is also not well reproduced. There is a possible effect from incomplete structure information and/or pre-equilibrium description. Looking at level production cross section would be helpful, but our data allow only the extraction of an upper limit.

    Five sets of data have been recorded with GRAPhEME, using ^{nat,182,182,184,186}W targets. This will allow to cross-check and normalize all the cross sections. In general, 10 to 15 transitions can be studied for each isotope. A covariant analysis is being developped to reflect the correlation between measurements. All this will produce a very rich and constraining set of experimental values to compare with models.

References

[1] A. Kerveno *et al.*, *EPJ Web of Conferences*, 42:01005, 2013.
[2] M. Kerveno *et al. Phys. Rev. C*, **87**:024609, Feb 2013.
[3] W.M. Haynes. CRC Handbook of Chemistry and Physics. Taylor & Francis, 2012.
[4] M.R. Gilbert *et al. Nuclear Fusion*, **52**(8):083019, 2012.
[5] P. Moller *et al. Atomic Data and Nuclear Data Tables*, **59**(2):185 – 381, 1995.

[6] John R. de Laeter *et al.* - Atomic weights of the elements. Review 2000 (IUPAC Technical report). 75, 2009.

[7] D. Lister, A. B. Smith, C. Dunford. *Phys. Rev.*, **162**:1077–1087, Oct 1967.

[8] Peter T. Guenther, Alan B. Smith, and James F. Whalen. *Phys. Rev. C*, **26**:2433–2446, Dec 1982.

[9] D. Tronc, J.M. Salomé, and K.H. Böckhoff. *NIM A*, **228**(2–3):217 – 227, 1985.

[10] D. Ene *et al.* *NIM A* **618**(1–3):54 – 68, 2010.

[11] J.C. Thiry. *Measurement of (n,xnγ) Reaction Cross Sections of Interest for the Generation IV Reactors*. PhD thesis, Université de Strasbourg, 2010.

[12] M. Mosconi *et al.* edited by E. Chiaveri (CERN, Geneva, Switzerland, 2010), September 2010.

[13] L. Arnold *et al.* In *Proc. 14th IEEE-NPSS Conf. on Real Time*, RTC'05, pages 265–269, Washington, DC, USA, 2005.

[14] C.R Brune. *NIM A*, **493**(1–2):106–110, 2002.

[15] L.C. Mihailescu, L. Oláh, C. Borcea, and A.J.M. Plompen. *NIM A*, **531**(3):375–91, 2004.

[16] Balraj Singh and Joel C. Roediger. Nuclear data sheets for a=182. *Nuclear Data Sheets*, **111**(8):2081 – 2330, 2010.

[17] Coral M. Baglin. Nuclear data sheets for a = 184. *Nuclear Data Sheets*, **111**(2):275 – 523, 2010.

[18] CORAL M. BAGLIN. Nuclear data sheets for a = 186. *Nuclear Data Sheets*, **99**(1):1 – 196, 2003.

[19] A.J. Koning and D. Rochman. *Nuclear Data Sheets*, **113**(12):2841 – 2934, 2012.

[20] A.J. Koning *et al.* TENDL-2014: TALYS-based evaluated nuclear data library, 2014.

[21] A. Bacquias *et al.* *NEA-NSC-DOC*, 2014:13, 2014.

[22] IAEA Nuclear Data Service Website, http://www-nds.iaea.org/exfor/